

Improvements in low-frequency foreground modeling for future primordial B-mode searches

Elena de la Hoz

April 4, 2022

Centre Pierre Binétruy (CNRS-UC Berkeley)



A little bit about myself

- ▶ Ph.D. at Instituto de Física de Cantabria (**IFCA**) in Santander.
- ▶ Worked mainly on **component separation** in the context of the **CMB**.
- ▶ Part of ELFS, LiteBIRD and QUIJOTE collaboration.
- ▶ Hired to work in **data analysis** for **CMB-S4**.



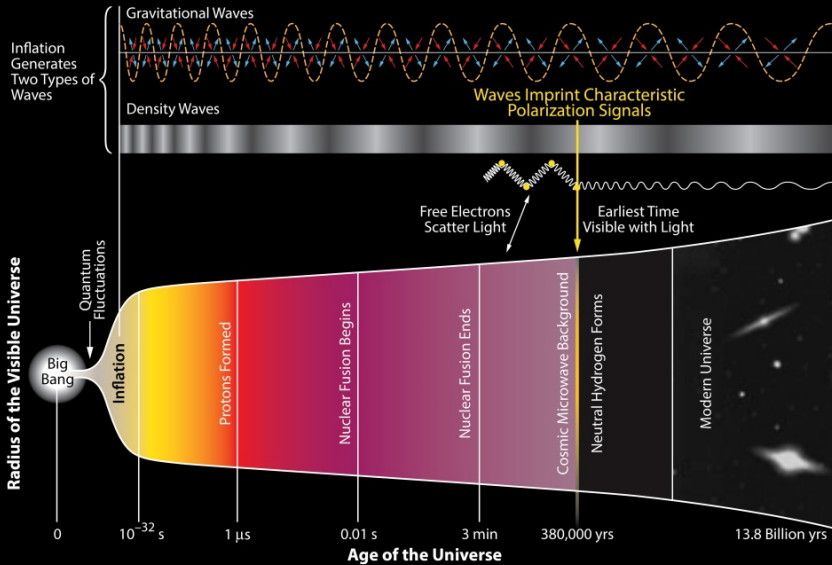
- ▶ Focused on:
 - ◇ **Low-frequency foregrounds** characterization.
 - ◇ **Forecast** on the detection of \mathbf{r} with **ELFS**.
 - ◇ Mitigation of **systematic effects**: non-perfect **calibration** of **polarization angles** and its connection to an **isotropic birefringence angle**.

Overview

- 1 Primordial B-modes
- 2 Synchrotron Emission
- 3 Synchrotron with QUIJOTE-MFI
- 4 ELFS Initiative
- 5 Take home messages

Primordial B-modes

History of the Universe



PGWs amplitude

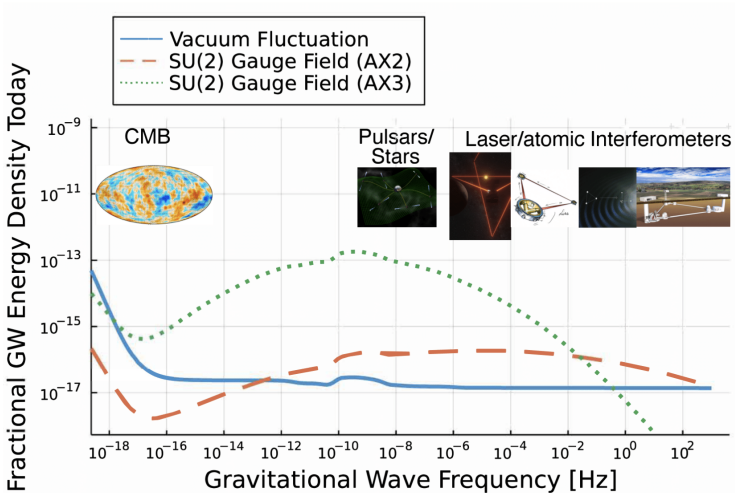


Fig. from **E. Komatsu 2202.13919**.

CMB B-modes

- ▶ Tensor fluctuations leave an **imprint** in the **B-mode** CMB power spectrum.
- ▶ The primordial B-mode signal is often parametrized with the **tensor-to-scalar ratio** r .
- ▶ Current best upper limit: $r < 0.032$, from BICEP/Keck+Planck+BAO **Tristram et al. 2112.07961**.
- ▶ Future experiments will target:
Simons Observatory: $r \simeq 0.003$,
LiteBIRD: $\sigma_r(r=0) = 1 \times 10^{-3}$,
CMB-S4: $\sigma_r(r=0) = 5 \times 10^{-4}$.

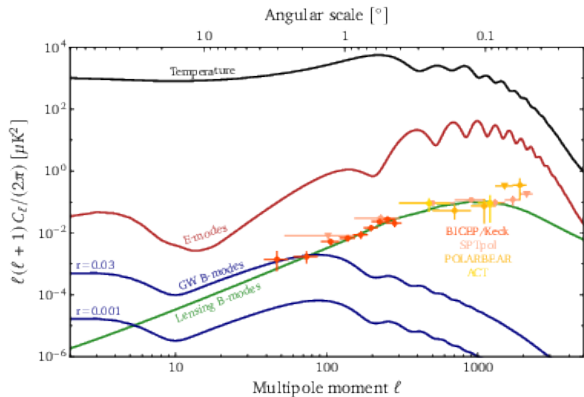


Fig. from **A. Achúcarro et al. 2203.08128**.

PGW detection challenges

▶ Lensed E- to B-modes:

- ▶ CMB photons experience multiple small local deflections by the matter distribution in their path toward us.
- ▶ Lensing leaks power from E- to B-modes.
- ▶ The lensing contribution behaves like white noise at $\ell \lesssim 1000$ of $\sim 5 \mu\text{K-arcmin}$.

▶ Systematic effects:

- ▶ Sensitivity of planned and future CMB experiments will reach unprecedented levels \rightarrow systematic errors will become a limiting factor regarding r detection.
- ▶ The list of known systematic effects is large and depend on the experimental design.

▶ Astrophysical foregrounds:

- ▶ Other physical mechanisms that emit in the microwave range.

Challenge: Astrophysical Foregrounds

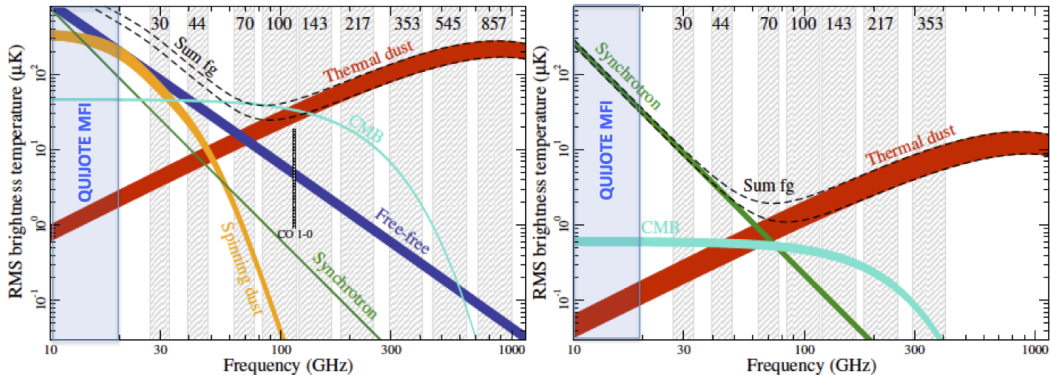


Fig. from **Radioforegrounds**

Challenge: Astrophysical Foregrounds

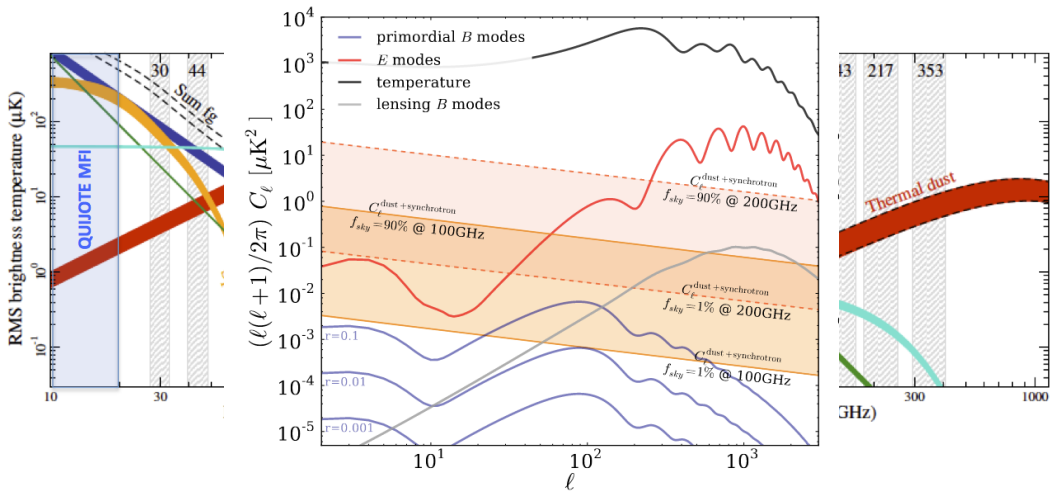


Fig. from J. Errard et al. 1509.06770

Synchrotron Emission

Synchrotron Emission

Synchrotron is generated by relativistic cosmic ray electrons spiraling around the Galactic magnetic field lines.

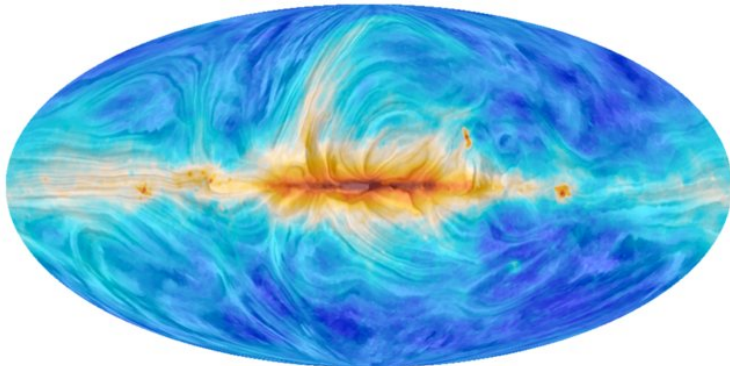


Fig. from *Planck* Collaboration [1502.01582](#).

Cosmic Rays Modeling (GALPROP)

Synchrotron is generated by relativistic cosmic ray electrons spiraling around the Galactic magnetic field lines.

Haslam et. al. 408 MHz Intensity map

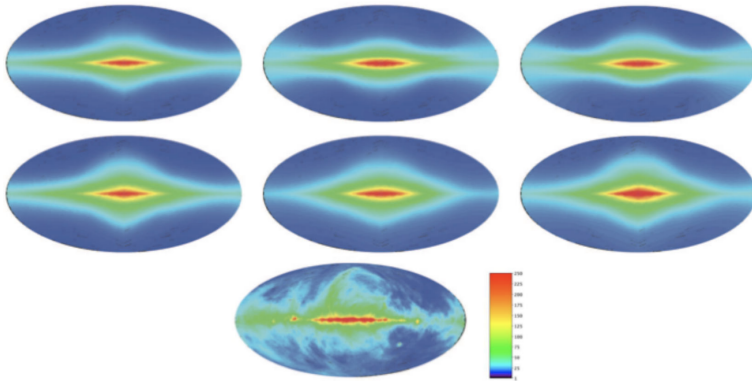


Fig. from **E. Orlando & A. Strong** 1309.2947.

Cosmic Rays Modeling (GALPROP)

Synchrotron is generated by relativistic cosmic ray electrons spiraling around the Galactic magnetic field lines.

WMAP 23 GHz Polarization Intensity map

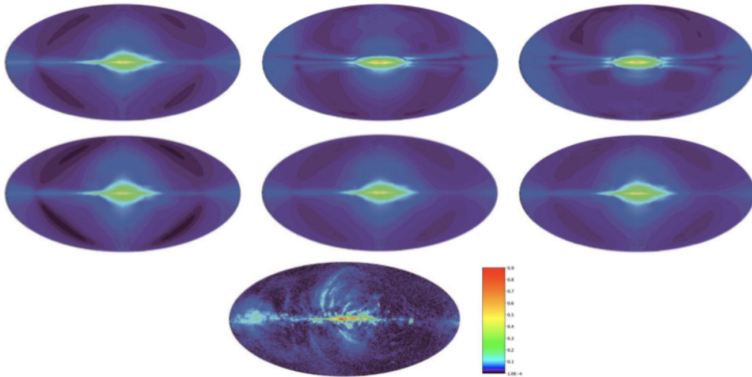


Fig. from **E. Orlando & A. Strong** [1309.2947](#).

Parametrization of the Synchrotron emission

Synchrotron is generated by relativistic cosmic ray electrons spiraling around the Galactic magnetic field lines.

- ▶ If the cosmic ray distribution is $N(E) \propto E^p$, the synchrotron SED is

$$S(\bar{n}) = A_s(\bar{n}) \left(\frac{\nu}{\nu_s} \right)^{\beta_s(\bar{n})}$$

- ▶ β_s has spatial and frequency variability. A model with curvature might be better:

$$S(\bar{n}) = A_s(\bar{n}) \left(\frac{\nu}{\nu_s} \right)^{\beta_s(\bar{n}) + c_s(\bar{n}) \log \frac{\nu}{\nu_s}}$$

Synchrotron with *Planck*

- ▶ Intensity model β_s with GALPROP prediction. Low-frequency foregrounds degeneracy.
- ▶ Polarization $\beta_s = -3.1$. S/N not sufficient to constrain this parameter.

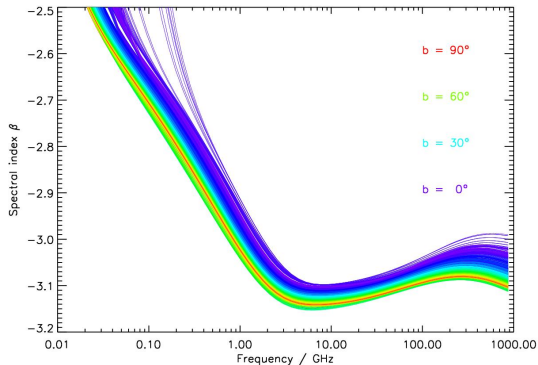


Fig. from *Planck* collaboration 1506.06660.

Ground-based experiments operating at low-frequencies

S-PASS

- ▶ 2.3 GHz
- ▶ Southern Hemisphere



C-BASS

- ▶ 5 GHz
- ▶ Both Hemispheres



QUIJOTE-MFI

- ▶ 10-20 GHz
- ▶ Northern Hemisphere



Synchrotron with S-PASS

- ▶ Polarized synchrotron emission compatible with a power law with $\beta_s = -3.22 \pm 0.08$.
- ▶ Synchrotron contamination in CMB B-modes is at the level of $r_{\text{synch}} \simeq 10^{-3}$.

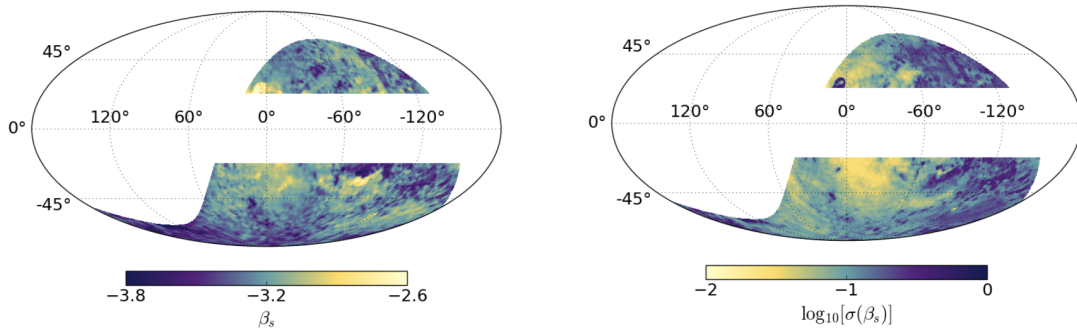


Fig. from **N. Krachmalnicoff et al.** [1802.01145](#).

Synchrotron with C-BASS

- ▶ From the intensity analysis found hints of curvature when comparing Haslam-C-BASS vs. Haslam-WMAP K ($\Delta\beta_s = 0.06 \pm 0.02$).
- ▶ From the polarization analysis they found larger spatial variations.

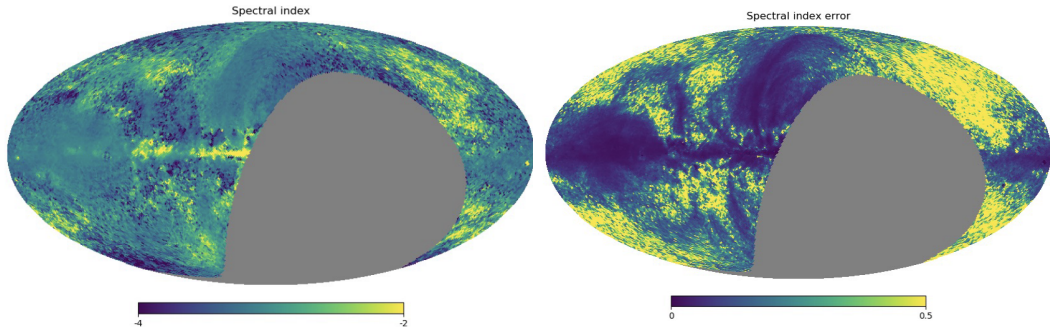


Fig. from **Angela Taylor**'s talk at *From Planck to the future of CMB*.

Synchrotron with QUIJOTE-MFI

QT1. Instruments

MFI,MFI2

11, 13, 17, 19 GHz

FWHM = 0.93° - 0.62°

MFI: 2012-2018

MFI2: 2022-

The QUIJOTE experiment

QT2. Instruments

TGI,FGI

30 and 40 GHz

FWHM = 0.37° - 0.28°

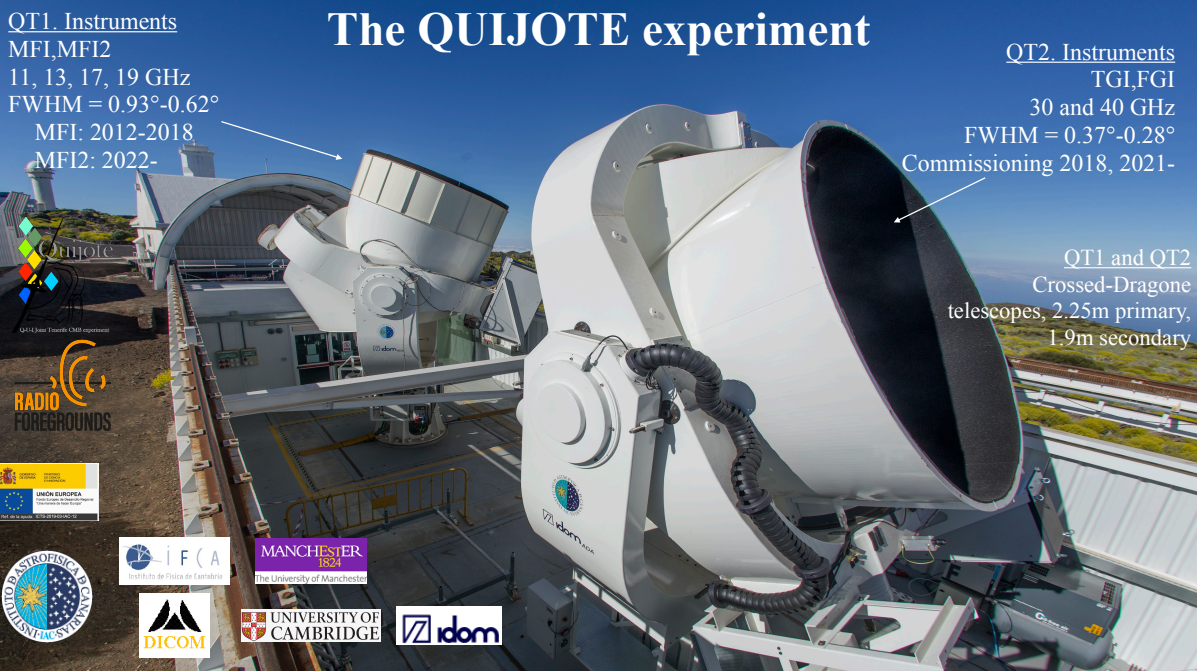
Commissioning 2018, 2021-

QT1 and QT2

Crossed-Dragnone
telescopes, 2.25m primary,
1.9m secondary

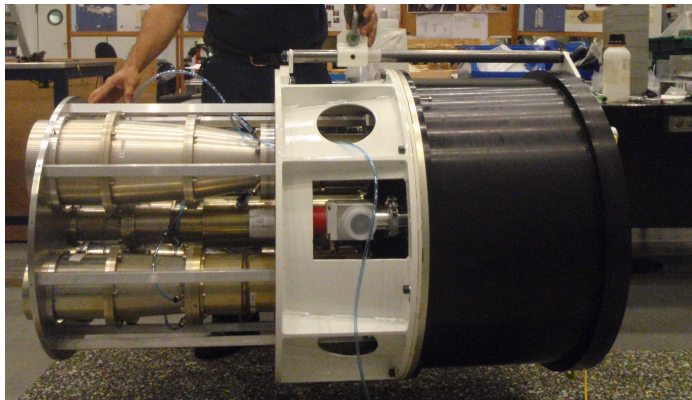


QJ14 Joint Institute CMS experiment



QUIJOTE-MFI

- ▶ Nov. 2012 - Oct. 2018.
- ▶ 10-20 GHz.
- ▶ 4 horns (polarimeters):
 - ◊ Horn 1 & 3: 10-14 GHz.
 - ◊ Horn 2 & 4: 16-20 GHz.
- ▶ 4 frequency channels:
11, 13, 17, 19 GHz.
- ▶ $\Delta\nu = 2$ GHz.
- ▶ Polarization sensitivity:
 $\sim 35\text{-}40\mu\text{K deg}^{-1}$.



QUIJOTE-MFI scientific results

MFI early results

- I. Intensity and polarization of the AME in the Perseus molecular complex (Génova-Santos et al. 2015).
- II. Polarization measurements in the Galactic MCs W43 and W47 and SNR W43 (Génova-Santos et al. 2017).
- III. Microwave spectrum of intensity and polarization in the Taurus MC complex and L1527 (Poidevin et al. 2019).

MFI wide survey

- IV. A northern sky survey at 10-20 GHz with the Multi-Frequency Instrument (Rubino-Marín et al. 2023).
- V. W49, W51 and IC443 SNRs as seen by QUIJOTE-MFI (Tramonte et al. 2023).
- VI. The Haze region and the Galactic Centre as seen by QUIJOTE-MFI (Guidi et al. 2023).
- VII. Galactic AME sources in the MFI wide survey (Poidevin et al. 2023).
- VIII. Component separation in polarization with the QUIJOTE-MFI wide survey. (de la Hoz et al. 2023).
- IX. Radio-sources in the QUIJOTE-MFI wide survey (Herranz et al. 2023).
- X. Spatial variability of AME parameters in the Galactic Plane (Fernández-Torreiro et al. submitted).
- XI. Polarised synchrotron loops and spurs. (Peel et al. in prep).
- XII. Analysis of the polarised synchrotron emission at the power spectrum level (Vansyngel et al. in prep).
- XIII. Intensity and polarization study of Supernova Remnants (López-Caraballo et al. in prep).
- XIV. The FAN region as seen by QUIJOTE-MFI (Ruiz-Granados et al. in prep).
- XV. The North Galactic Spur as seen by QUIJOTE-MFI (Watson et al. in prep).
- XVI. Component separation in intensity with the QUIJOTE-MFI wide survey (de la Hoz et al. in prep).

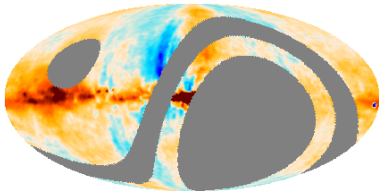
Published
in MNRAS

Other MFI papers

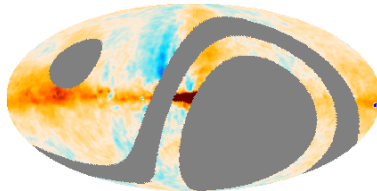
- ◇ Detection of spectral variations of AME with QUIJOTE and C-BASS (Cepeda-Arroita et al. 2021).
- ◇ The PICASSO map-making code: application to a simulation of the QUIJOTE MFI survey (Guidi et al. 2021).
- ◇ Searching for dark-matter waves with PPTA and QUIJOTE pulsar polarimetry (Castillo et al. 2022).
- ◇ MFI data processing pipeline (Genova-Santos et al. in prep).

Sky Signal Maps I. QUIJOTE-MFI

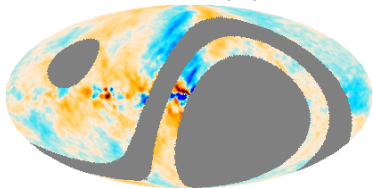
11 GHz (Q)



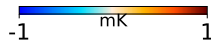
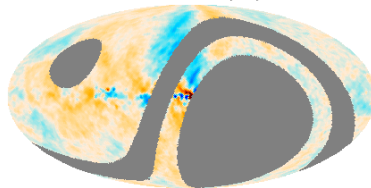
13 GHz (Q)



11 GHz (U)



13 GHz (U)



Wide survey: $\sim 51\%$ of sky. 52 arc min resolution.

Sky Signal Maps II. Ancillary Data

Planck

- PR4 (NPIPE).
- Pol. LFI: 30, 44, 70 GHz.
- Pol. HFI: 100, 143, 217 and 353 GHz.

WMAP

- Polarized 9-year maps.
- K and Ka (22.8 and 33.1 GHz) bands.



All maps have:

- $N_{side} = 64$.
- $FWHM = 2$ deg.
- Color corrections w/ `fastcc`.

Covariance matrices

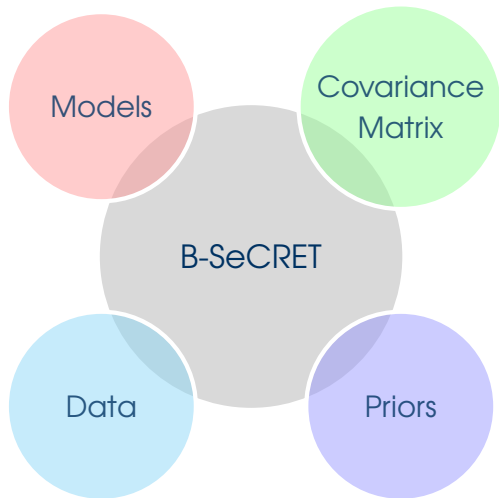
- Among frequency detectors.
- From noise simulations.
- 11 and 13 GHz are correlated.
- The rest are independent.

Component Separation Methodology. B-SeCRET

B-SeCRET

- ◇ Bayesian
- ◇ Parametric
- ◇ Maximum likelihood
- ◇ MCMC

E. de la Hoz et al. 2002.12206



Polarized Sky Components: Models

Synchrotron

Power law model:

$$\begin{bmatrix} \mathbf{a}_s^Q \\ \mathbf{a}_s^U \end{bmatrix} \left(\frac{\nu}{\nu_s} \right)^{\beta_s}$$

Power law with curvature model:

- Uniform curvature.
- Spatially varying curvature.

$$\begin{bmatrix} \mathbf{a}_s^Q \\ \mathbf{a}_s^U \end{bmatrix} \left(\frac{\nu}{\nu_s} \right)^{\beta_s + \mathbf{c}_s(\nu/\nu_s)}$$

CMB

Black-body model:

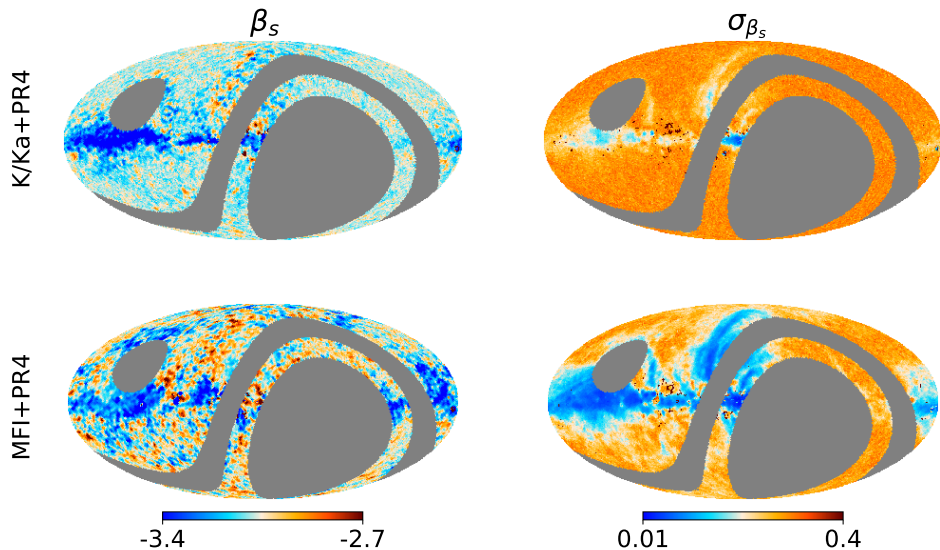
$$\begin{bmatrix} \mathbf{c}^Q \\ \mathbf{c}^U \end{bmatrix} \frac{x^2 e^x}{(e^x - 1)^2}$$

Thermal Dust

Modified black-body model:

$$\begin{bmatrix} \mathbf{a}_d^Q \\ \mathbf{a}_d^U \end{bmatrix} \left(\frac{\nu}{\nu_d} \right)^{\beta_d - 2} \frac{B(\nu, \mathbf{T}_d)}{B(\nu_d, \mathbf{T}_d)}$$

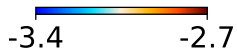
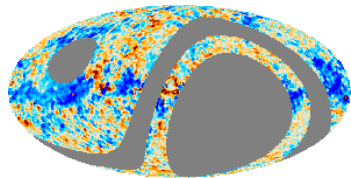
Synchrotron's Spectral Index I. Datasets



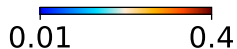
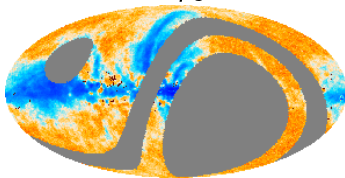
Synchrotron's Spectral Index I. Datasets

MFI+K/Ka+PR4

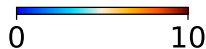
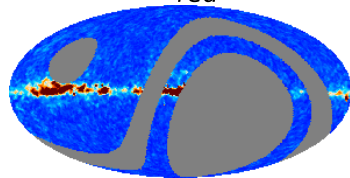
β_s



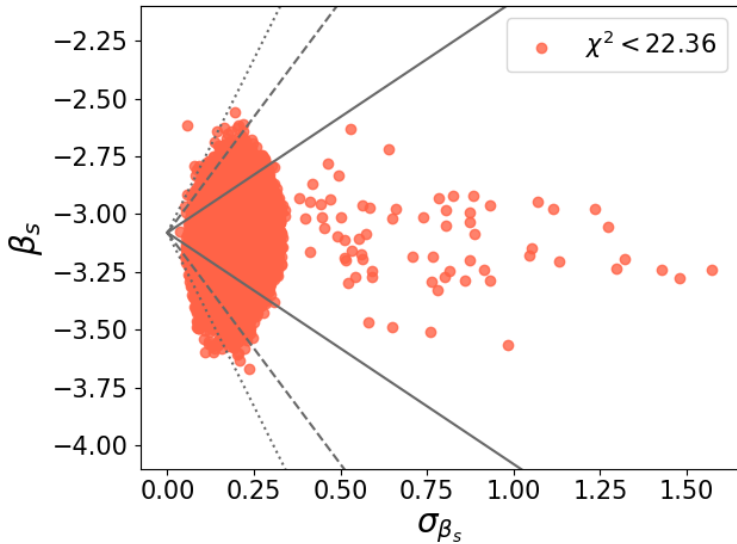
σ_{β_s}



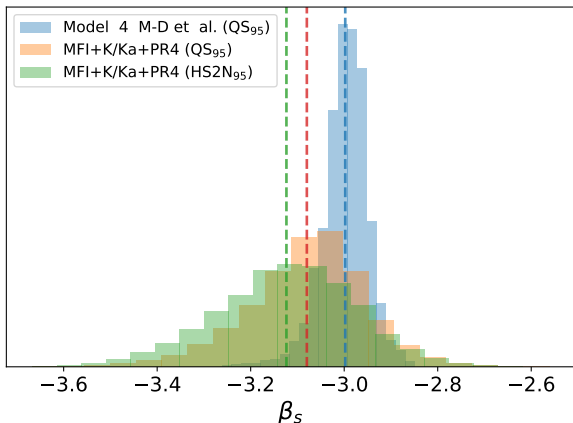
χ^2_{red}



Synchrotron's Spectral Index II. Spatial Variability

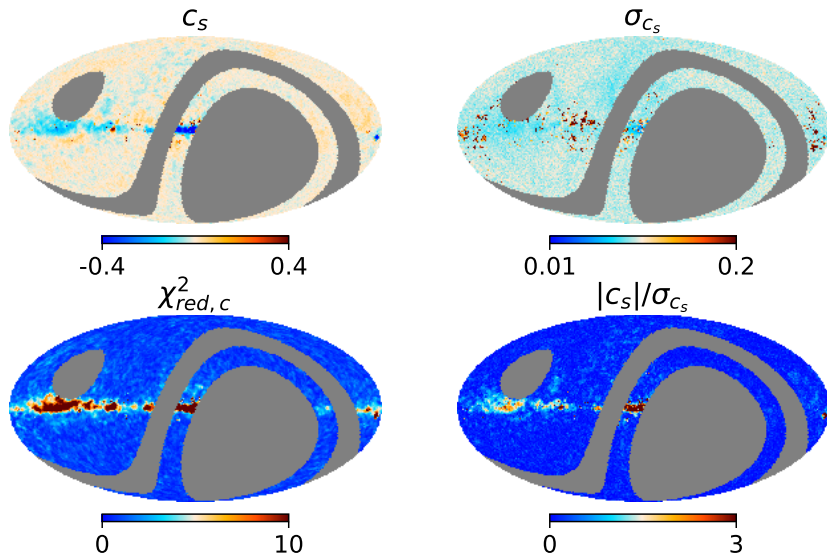


Synchrotron's Spectral Index III. Comparison with other β_s templates

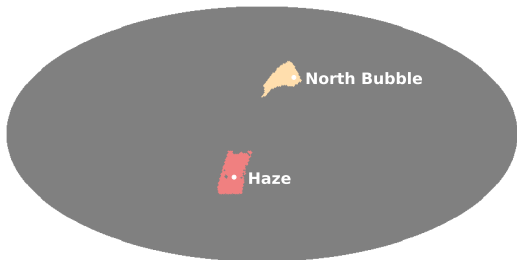
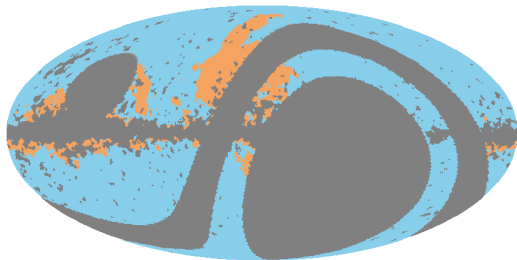


- ▶ Only pixels whose χ^2 is at 95% confidence.
- ▶ MFI+K/Ka+PR4: $\mathcal{N}(-3.08, 0.13^2)$.
- ▶ PySM: $\mathcal{N}(-3.00, 0.05^2)$.
- ▶ $\frac{\sigma_{\beta_s}(\text{MFI} + \text{K/Ka} + \text{PR4})}{\sigma_{\beta_s}(\text{PySM})} \sim 2.6$.

Curvature I. Power law with Spatially Varying Curvature



Curvature II. Power law with Uniform Curvature



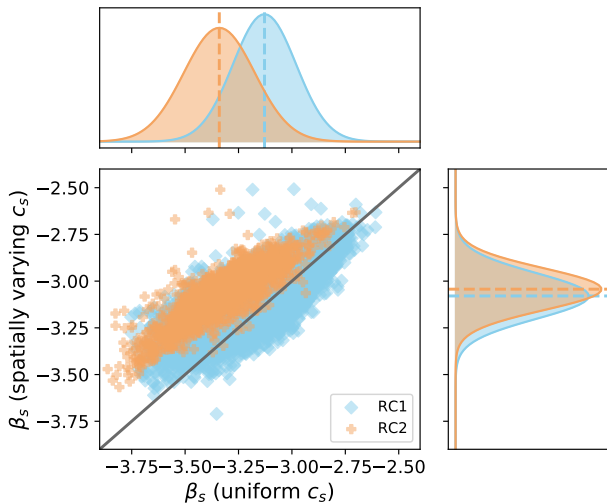
Region	c_s^R	$\sigma_{c_s^R}$	$ c_s^R / \sigma_{c_s^R}$
RC1	-0.0797	0.0012	63.75
RC2	-0.2768	0.0017	161.57
Haze	0.041	0.010	4.23
North bubble	-0.083	0.007	11.43



Not statistical significant results to elucidate which model agrees better with the data.

F. Guidi et al. [2301.05115](#)

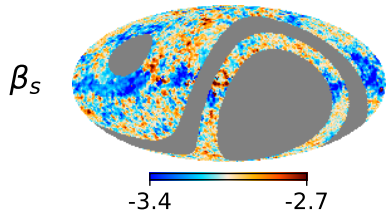
Curvature III. Recovered β_s with spatially varying and uniform curvature



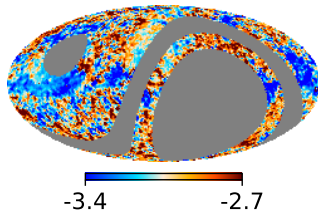
β_s and c_s are not independent. Either more sensitive data at the QUIJOTE frequencies or data at lower frequencies are required to break the degeneracy.

Robustness with respect to the Prior Information

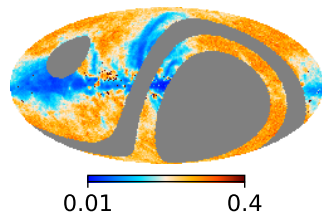
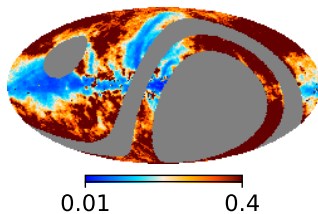
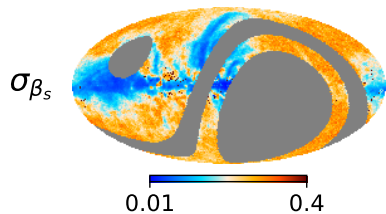
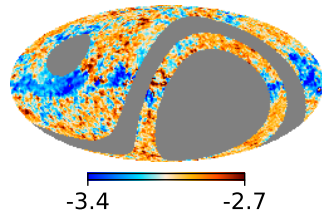
$\mathcal{N}(-3.1, 0.3)$



$\mathcal{N}(-3.1, 0.6)$

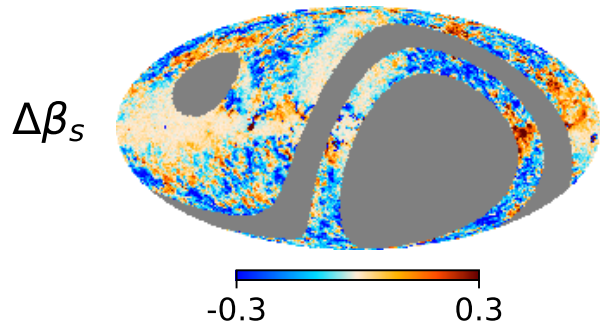


$\mathcal{N}(-3.0, 0.3)$

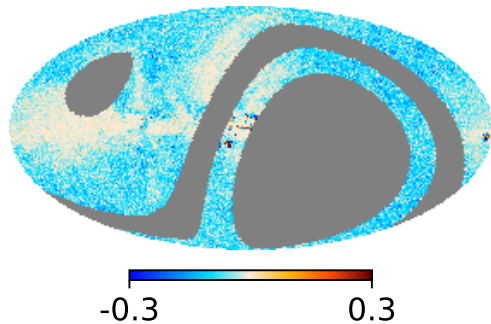


Robustness with respect to the Prior Information

$\mathcal{N}(-3.1, 0.6)$



$\mathcal{N}(-3.0, 0.3)$







Summary

- ▶ **QUIJOTE-MFI** data **improves** significantly the β_s **characterization**.
- ▶ We find statistically **significant** β_s **spatial variability** across the sky.
- ▶ Current models might **underestimate** the **dispersion** of the synchrotron's spectral parameter.
- ▶ The **synchrotron models** considered **fit well** the data **outside the galactic plane**.
- ▶ We **detect uniform curvature**.
- ▶ Results **not robust** enough to determine which **model is favoured**.
- ▶ β_s estimation is **prior independent** in the **high signal-to-noise synchrotron** regions.

ELFS Initiative

European Low-Frequency Survey

- ▶ European Initiative to measure the **low-frequency** microwave sky from **ground**.
- ▶ Main **participants**:
 -  France (IRAP).
 -  Italy (SISSA and University of Milan).
 -  Spain (IAC and IFCA).
 -  U.K (University of Oxford).
- ▶ Two **strategies** considered:
 - ◇ **Ambitious**: measure from **both hemispheres** the frequency range **10-120 GHz** with a enough sensitivity to obtain $\sigma_r \lesssim 10^{-3}$.
 - ◇ **Economic**: be a **complement** to other CMB experiments by helping constrain the low-frequency foregrounds (**10-40 GHz**).
- ▶ Initial exploratory study by **E. de la Hoz et al. 2002.12206**.

Instrumental setup

Three frequency **bands** (set by atmosphere):

- ▶ Low-frequency (lb): 10-20 GHz.
- ▶ Medium-frequency (mb): 26-46 GHz.
- ▶ High-frequency (hb): 75-120 GHz.

Studied optimal # of channels per band.

Default: (10,10,15)

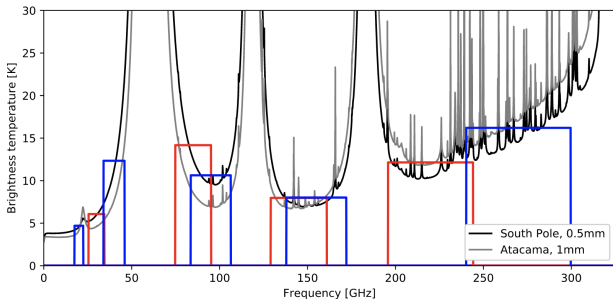


Fig. from **CMB-S4 collaboration 2008.12619**



Stopping at 120 GHz allow us to study only the **Rayleigh-Jeans** part of the thermal dust. Thus, we avoid possible **biases** due to **incorrect modeling**.

M. Remazeilles et al. 1509.04714, B. Hensley et al. 1709.07897.

Observational strategies – Sky coverage

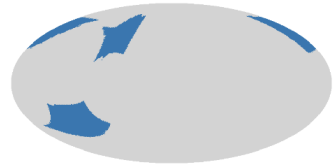
Three different sky **strategies** considered:



(a) Planck: 70% galactic plane mask



(b) QUIJOTE: Wide Survey



(c) QUIJOTE: Cosmological areas

- (a) Default: **Two** experiments, one in each **Hemisphere** (e.g., at Atacama and Tenerife).
- (b) One experiment in the **Northern Hemisphere** with a **wide survey**.
- (c) One experiment in the **Northern Hemisphere** focused on **specific areas**.

Signal map simulations

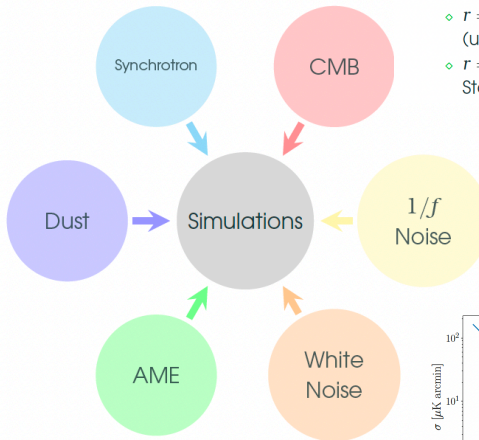
Foregrounds:

$$\text{Synch.:} \begin{bmatrix} \mathbf{a}_s^{\text{Q}} \\ \mathbf{a}_s^{\text{U}} \end{bmatrix} \left(\frac{\nu}{\nu_s} \right)^{\beta_s + \mathbf{c}_s (\nu / \nu_{cs})}$$

$$\text{Dust:} \begin{bmatrix} \mathbf{a}_d^{\text{Q}} \\ \mathbf{a}_d^{\text{U}} \end{bmatrix} \left(\frac{\nu}{\nu_d} \right)^{\beta_d}$$

$$\text{AME:} \begin{bmatrix} \mathbf{a}_a^{\text{Q}} \\ \mathbf{a}_a^{\text{U}} \end{bmatrix} \left(\frac{\nu}{\nu_a} \right)^{\beta_a + \mathbf{c}_a (\nu / \nu_{ca})}$$

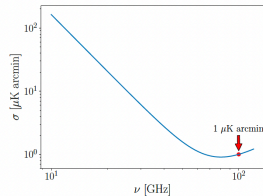
- ▶ Foregrounds are generated and fitted with the same model.
- ▶ Pixelwise fit.
- ▶ Joint probability.



▶ Two tensor-to-scalar ratio considered:

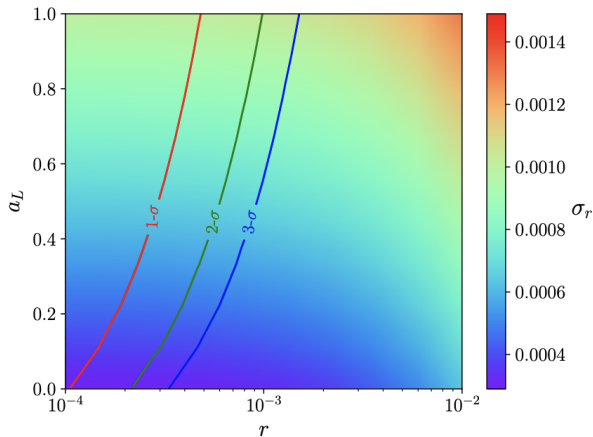
- ◊ $r = 0$: no primordial B-modes (upper limit).
- ◊ $r = 3.7 \cdot 10^{-3}$ compatible with Starobinsky's model.

$$N_\ell = N_w + N_{\text{corr}} \left(\frac{\ell}{\ell_{\text{knee}}} \right)^\gamma$$



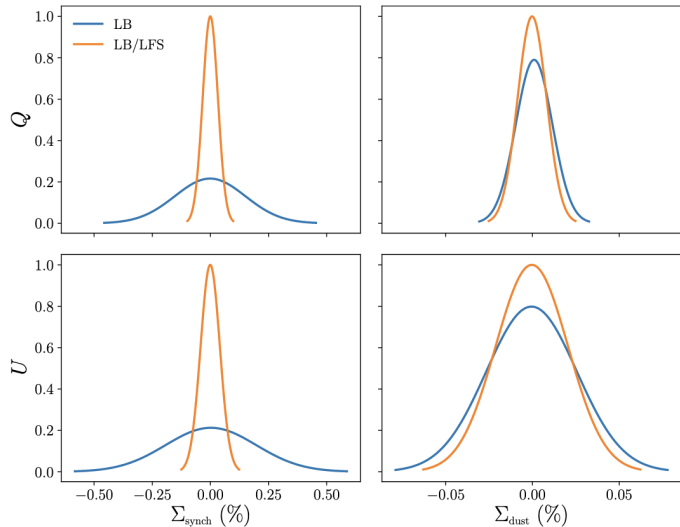
Ambitious proposal: Detection of the tensor-to-scalar ratio

- ▶ An experiment with **two experiments** one in the Northern Hemisphere and the other in the Southern can reach sensitivities of $\sigma_r \sim \mathbf{10^{-3}}$.
- ▶ This **sensitivity worsens** when considering just **one experiment** on the Northern Hemisphere in both cases.
- ▶ Including **delensing** techniques can help reduce σ_r more than a more sensitive experiment.



Economic proposal: Improvement of Foreground characterization

- ▶ This type of experiment is a great **complement** to other missions such as **LifeBIRD**.
- ▶ Only using lb and mb (**10-40 GHz**).
- ▶ The combination of data lead to a **significant improvement** of the **synchrotron** characterization and **slight improvement** in the **thermal dust**.



ELFS-S status

- ▶ Proposal to **replace** the **Simons Array's (SA's) 220/280 GHz** receiver with a **Europe-supplied 6-12 GHz** receiver.
- ▶ Plan is to install a **C-BASS-like 6-12 GHz** receiver first, and add a second Europe-supplied receiver from **10-20 GHz (QUIJOTE MF12)** later.
- ▶ **Better combination** between **SA** and **SO**, since SO will have a SAT at 220/280 GHz.

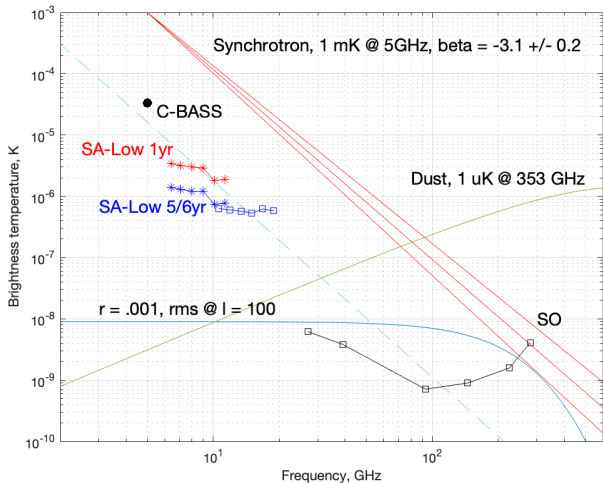


Fig. from **Mike Jones** (Oxford)

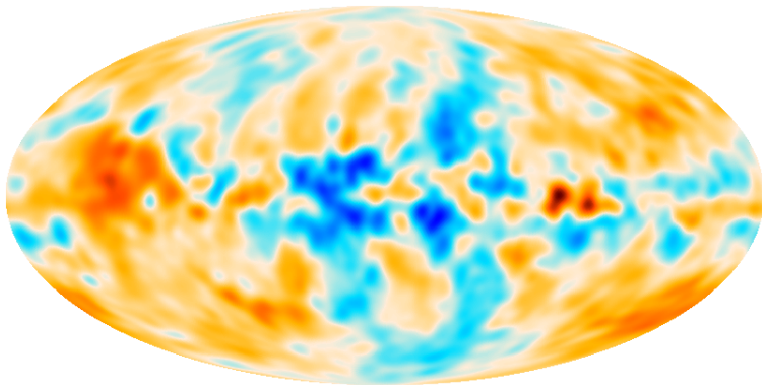
Take home messages

Take home messages

- ▶ The **characterization** of astrophysical **foregrounds** is **crucial to** remove them properly from the signal sky maps and **detect primordial B-modes**.
- ▶ Planned CMB experiments include several bands to explore the complexity of the thermal dust. However, the **synchrotron** emission might be more **complicated** than expected and **hinder** our attempts of **detecting r** .
- ▶ The **QUIJOTE-MFI** instrument data help **improvement** significantly with the **characterization** of the **synchrotron** emission and shows **hints** of it being more **complex** than previously thought.
- ▶ Initiatives like **ELFS** have shown that a **low-frequency** instrument can reach **sensitivities** on the order of $\sigma_{\tau} \sim 10^{-3}$ or help **characterize** the **low-frequency foregrounds** which is mandatory for a **robust detection claim**.

Back-up

Simulation codes' synchrotron's spectral index template



M.-A. Miville-Deschenes et al. 0802.3345

RFI correction. Function of the Declination (FDEC)

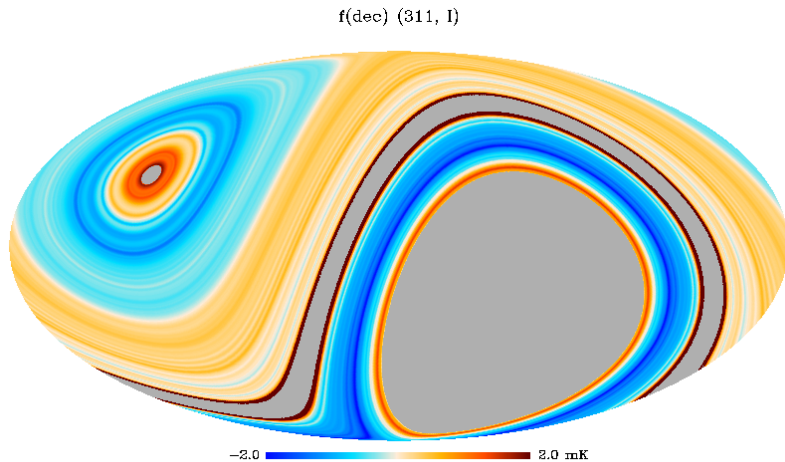


Figure from **J. A. Rubiño-Martín** et al., 2022, MNRAS, submitted.

RFI correction. Function of the Declination (FDEC)

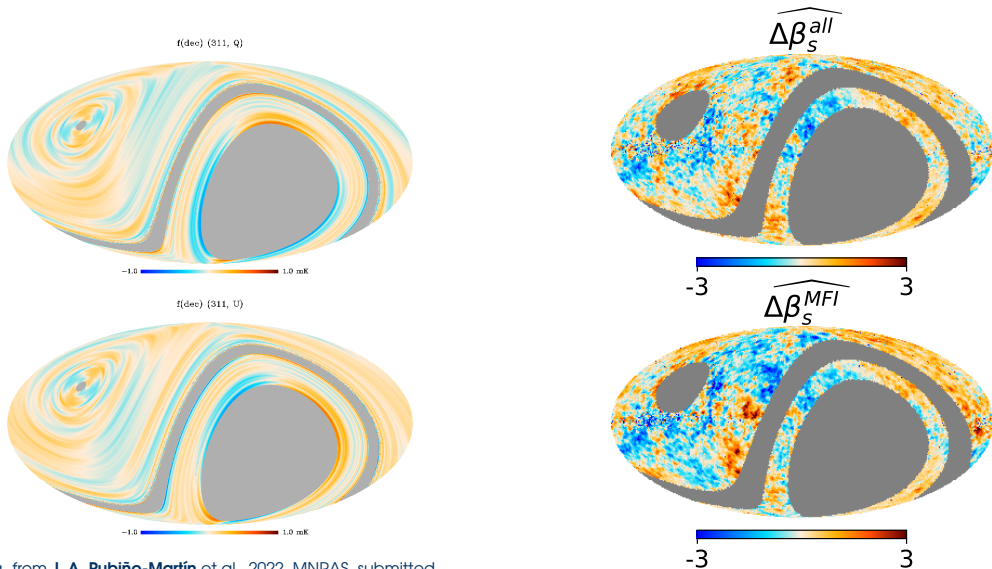


Fig. from J. A. Rubiño-Martín et al., 2022, MNRAS, submitted.

Covariance Matrices and Instrumental Effects

Covariance matrices

- Covariance among frequency detectors per pixel.
- Calculated from noise simulations.
- 11 and 13 GHz channels are correlated.
- The rest are assumed independent.

Noise simulations

- **QUIJOTE**: Collaboration noise simulations.
- **WMAP**: white noise simulations.
- **Planck**: Available noise simulations for PR3 and PR4.

Detectors response

Colour corrections with `fastcc`.

Polarized Sky Components II. Priors

Synchrotron

Power law model:

$$\beta_{\mathbf{s}} \in \mathcal{N}(-3.1, 0.3)$$

Power law with curvature model:

- Uniform curvature.
- Spatially varying curvature.

$$\beta_{\mathbf{s}} \in \mathcal{N}(-3.1, 0.3)$$

$$\mathbf{c}_{\mathbf{s}} \in \mathcal{N}(0, 0.1)$$

CMB

Black-body model:

None

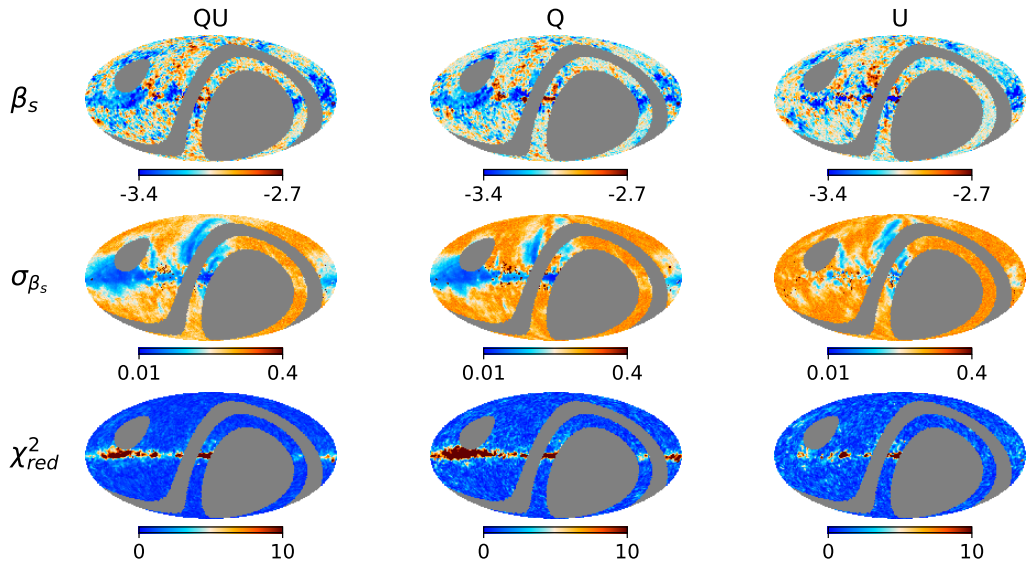
Thermal Dust

Modified black-body model:

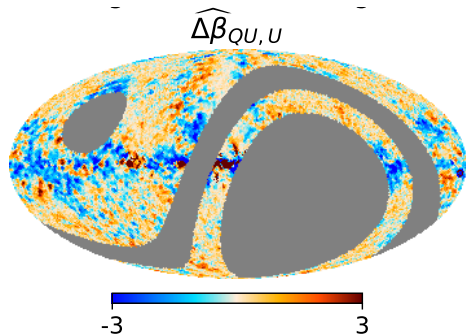
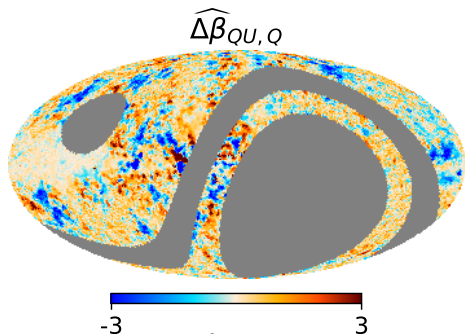
$$\beta_{\mathbf{d}} \in \mathcal{N}(1.55, 0.1)$$

$$\mathbf{T}_{\mathbf{d}} \in \mathcal{N}(21, 3)$$

Synchrotron Spectral Index from Independent Q and U analysis I

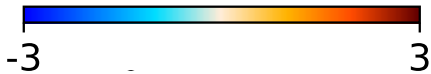
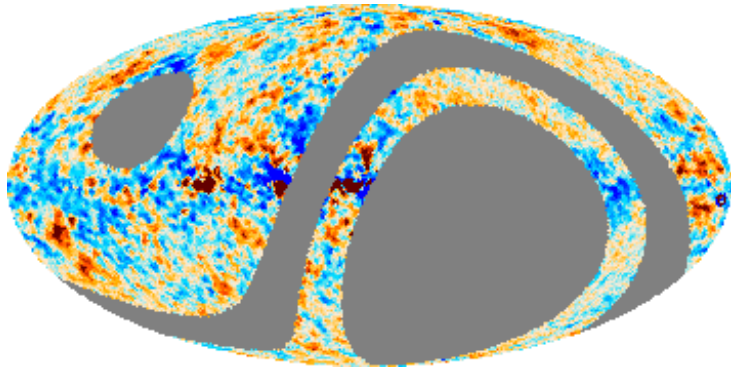


Synchrotron Spectral Index from Independent Q and U analysis II

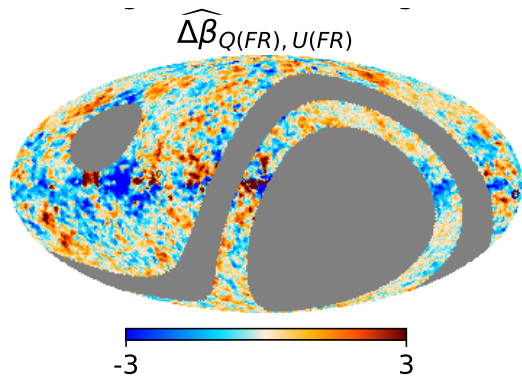
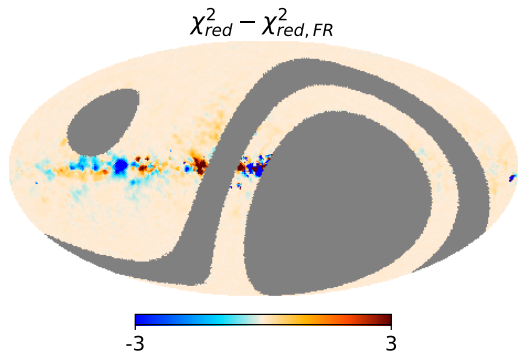


Synchrotron Spectral Index from Independent Q and U analysis III

$$\widehat{\Delta\beta}_{Q,U}$$



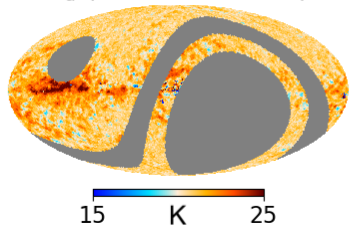
Faraday Rotation



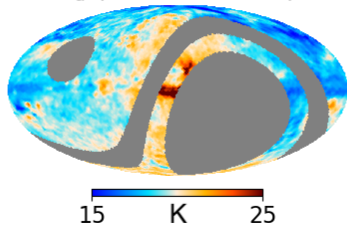
S. Hutschenreuter et al. [2102.01709](#)

Thermal Dust Temperature

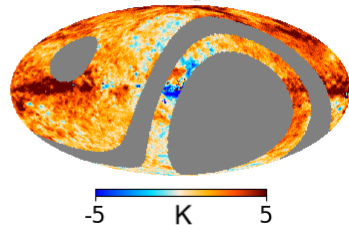
T_d (MFI+K/Ka+PR4)



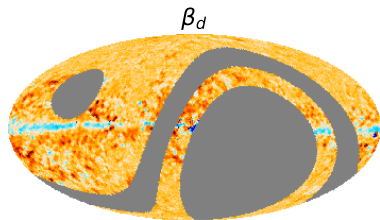
T_d (Commander I)



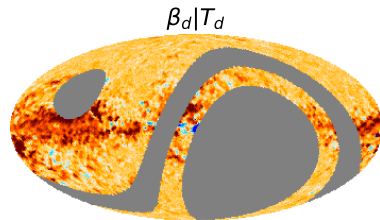
ΔT_d



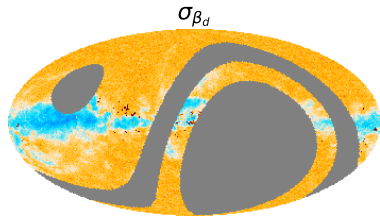
Thermal Dust Spectral Index



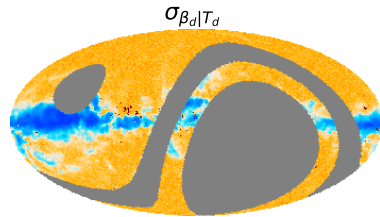
1.3 1.7



1.3 1.7



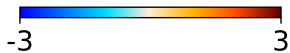
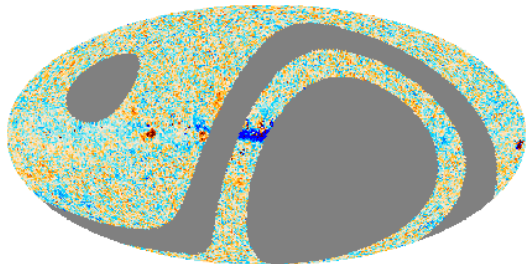
0.001 0.15



0.001 0.15

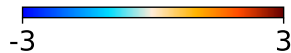
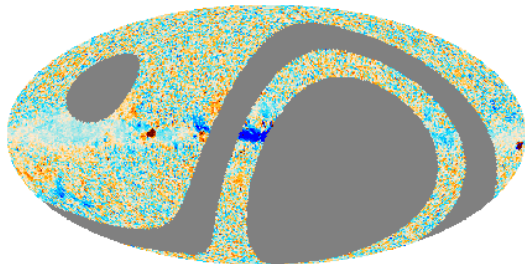
Spectral indices differences II. MFI+K/K α +PR4 vs. K/K α +PR4

$\widehat{\Delta\beta}_d$



Free T_d

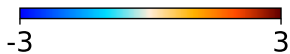
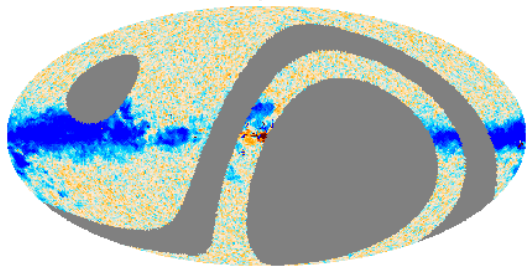
$\widehat{\Delta\beta}_d$



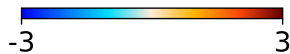
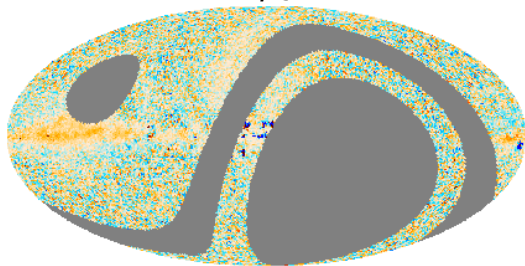
Fixed T_d

Spectral indices differences I. Free vs. fixed T_d parameter

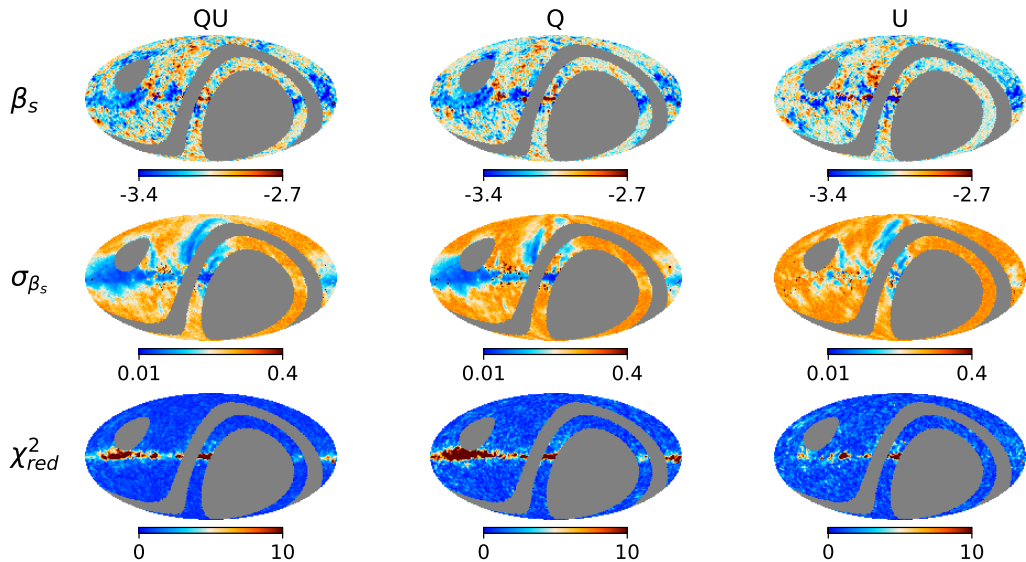
$\widehat{\Delta\beta_d}$



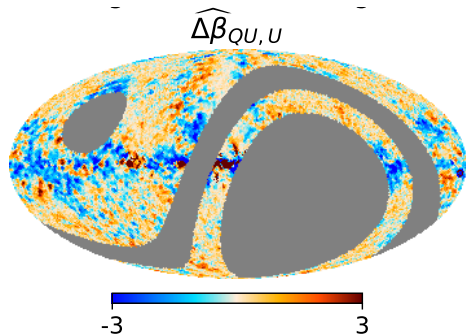
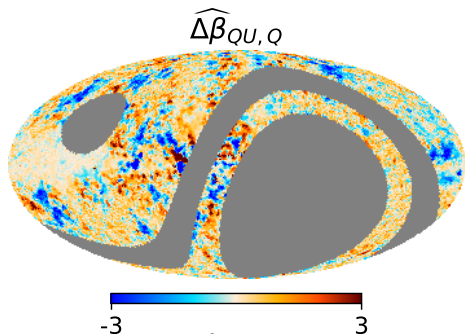
$\widehat{\Delta\beta_s}$



Synchrotron Spectral Index from Independent Q and U analysis I

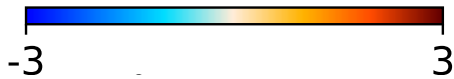
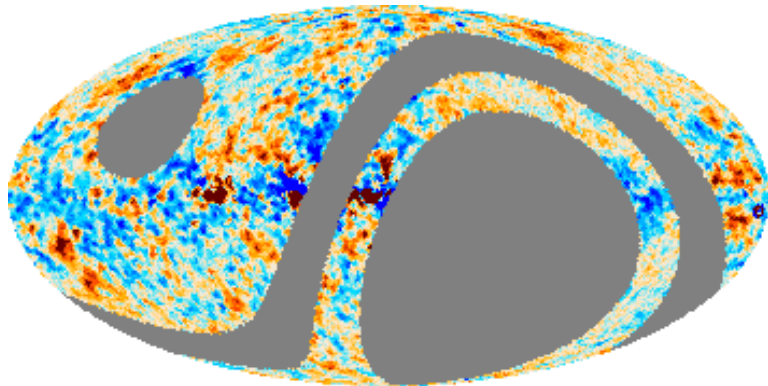


Synchrotron Spectral Index from Independent Q and U analysis II

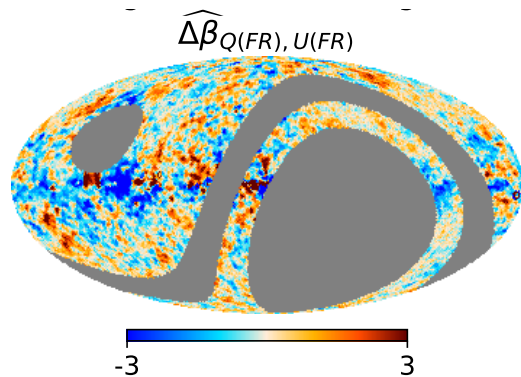
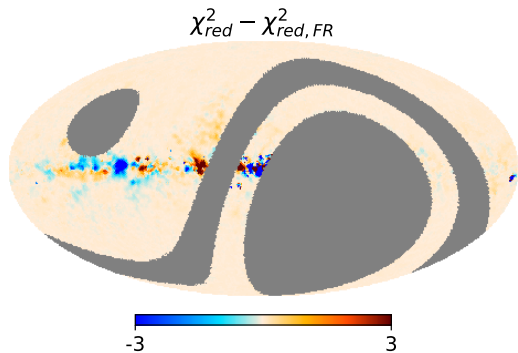


Synchrotron Spectral Index from Independent Q and U analysis III

$$\widehat{\Delta\beta}_{Q,U}$$

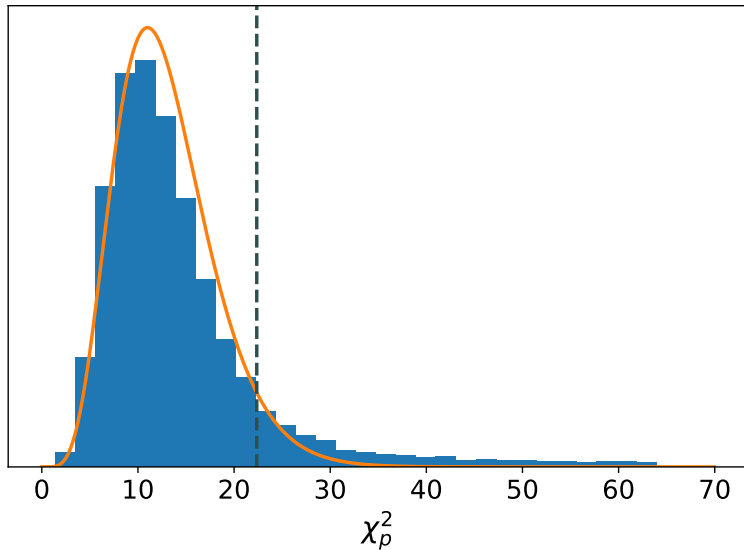


Faraday Rotation

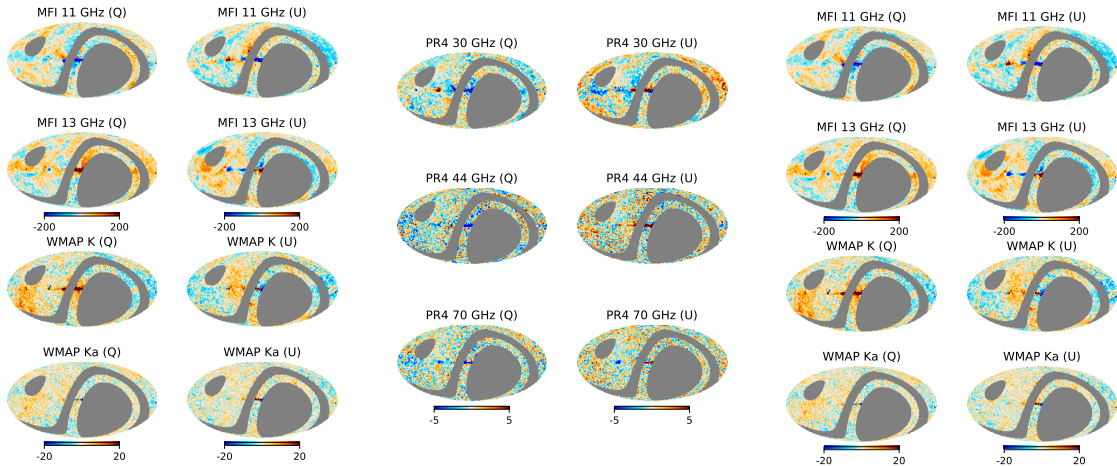


S. Hutschenreuter et al., 2021, arXiv:2102.01709.

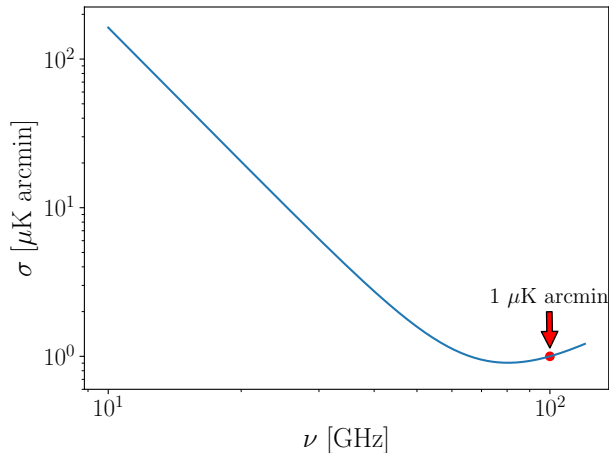
χ^2 distribution



Residuals maps



Proposed Experiment. Sensitivity



- ▶ Mimics the frequency dependence of the major contaminants: synchrotron and thermal dust
- ▶ 1 μK arc min @ 100 GHz.
- ▶ synch. contribution = dust contribution @ 70 GHz
- ▶ In the default case we considered (10,10,15) channels per band.

LiteBIRD

- ▶ Lite (Light) satellite for the study of B-mode polarization and Inflation from cosmic background Radiation Detection.
- ▶ JAXA's L-class mission selected in May 2019
- ▶ Expected launch in late 2029.
- ▶ All-sky 3-year survey, from Lagrangian point L2.
- ▶ Large frequency coverage (40–402 GHz, 15 bands)
- ▶ 70–18 arcmin angular resolution.
- ▶ Final combined sensitivity: $2.2 \mu\text{K}\cdot\text{arcmin}$.

